

SEP 15 1953



NACA

# RESEARCH MEMORANDUM

PRELIMINARY INVESTIGATION OF THE EFFECTS OF CASCADING  
ON THE OSCILLATING LIFT FORCE OF AN AIRFOIL  
VIBRATED IN BENDING

By Donald F. Johnson and Alexander Mendelson

Lewis Flight Propulsion Laboratory  
Cleveland, Ohio

NATIONAL ADVISORY COMMITTEE  
FOR AERONAUTICS

WASHINGTON  
September 9, 1953



3 1176 01435 2646

NACA RM E53F29

NATIONAL ADVISORY COMMITTEE FOR AERONAUTICS

RESEARCH MEMORANDUM

PRELIMINARY INVESTIGATION OF THE EFFECTS OF CASCADING  
ON THE OSCILLATING LIFT FORCE OF AN AIRFOIL  
VIBRATED IN BENDING

By Donald F. Johnson and Alexander Mendelson

SUMMARY

Measurements were made of the oscillatory lift force acting on an airfoil vibrated in bending. Results were obtained for an isolated airfoil and for the same airfoil oscillated in a cascade, at low and high angles of attack. It was found that at high angles of attack and at low values of the reduced frequency, the damping for the isolated airfoil can become negative. The oscillating lift force changes little, for the case considered, by placing this blade in a stationary cascade. It is indicated that for this case the effect of the cascade is generally to increase the damping by a slight amount.

INTRODUCTION

Blade vibrations at stalling angles are becoming an increasingly important problem in the operation of axial-flow compressors and turbines. Numerous recent failures of jet engines have been attributed to compressor-blade vibrations at stall.

In many cases, compressor-blade vibration has been attributed to stalling flutter occurring as a result of hysteresis or a phase lag between the lift force and the angle of attack of the airfoil (refs. 1 and 2). This has generally resulted in pure bending vibrations at the natural frequency of the blade. There is one case where severe bending oscillations attributed to hysteresis were encountered with an isolated blade operating at several degrees above stall (ref. 3). A cascade of blades in a tunnel may also flutter in bending as in reference 4. Furthermore, the authors of reference 4 attempt to show theoretically that if a blade in a cascade oscillates harmonically, "the variation of the mean air velocity allows for an exchange of energy such that the blade absorbs work supplied by the air stream."

In order to determine some of the basic effects of high angles of attack, the oscillatory aerodynamic lift and moment for an isolated airfoil, oscillating in torsion and translation, were measured and are reported in reference 2.

2939

CD-1

The present preliminary investigation was made at the NACA Lewis laboratory to measure experimentally the oscillatory aerodynamic lift at low and high angles of attack of an airfoil oscillating in translation, with the airfoil isolated and in a stationary cascade. In this way, the effect of cascading on the oscillatory aerodynamic lift of an airfoil oscillating in translation was determined. Incidentally, it was possible to investigate the conclusions of reference 4 that such an airfoil would be more prone to flutter than an isolated airfoil.

#### APPARATUS

The apparatus used in this investigation was similar in principle to that of reference 2. It consisted of a model airfoil supported at one end by a cantilever equipped with strain gages. This airfoil was driven in a "flapping" motion in an air stream, and the oscillatory lift force was measured by the strain gages and recorded.

A photograph of the linkage of the flutter engine which is used to drive the airfoil in bending is shown in figure 1. The linkage to drive the airfoil in torsion (shown to the left) was not used in this investigation.

Displacement pickup. - The displacement disk (fig. 1) was rigidly attached to the flywheel. There was a 1/4-inch-diameter hole close to the rim of the disk. A spotlight and a shielded photoelectric cell were arranged on opposite sides of the disk. Once each revolution, the light actuated the cell through the hole. The displacement trace was recorded on one channel of the recording oscillograph, which was wired in series with the photoelectric cell and a 90-volt battery.

Airfoil. - Inertia loads were kept as low as possible by using a laminated basswood airfoil. As is shown in figure 2, the aluminum airfoil shaft passed through the airfoil and was secured with a nut on the outside end. The shaft was keyed at both ends in 1/16-inch-thick aluminum plates which were screwed and cemented to the airfoil. The inside end of the airfoil shaft terminated in a slotted cylinder which fit snugly over the rocker-arm shaft just beyond the strain gages, the slots allowing the angle of attack of the airfoil to be varied from  $-5^{\circ}$  to  $45^{\circ}$ . The airfoil section had the coordinates of the M.I.T. "sharp" airfoil (ref. 2) which was approximately 12 percent thick and had a chord of 4 inches and a span of  $8\frac{1}{2}$  inches.

The cascade blades were of NACA 0015 cross section. They were machined from 24S-T aluminum and were rigidly fastened at both ends to the tunnel walls. The gap chord ratio was  $1/2$  and the stagger was zero.

Rocker arm and strain gages. - The rocker arm and the pillow block were made in one piece of 24S-T aluminum. The outside end of the rocker arm beyond the pillow block was of 7/16- by 7/16-inch square cross section; on its upper and lower surfaces were mounted four active wire-resistance strain gages with their elements running lengthwise. These gages composed the four legs of a bridge that was used in the conventional way to indicate bending strain and hence lift force on the rocket arm.

When the flutter engine drives an airfoil in an air stream, the force indicated by the strain gages consists of two parts: (1) the inertia force and (2) the oscillatory lift force. Because of the comparatively small magnitude of the lift force, it is desirable to subtract the inertia force electronically. Therefore, strain gages were placed on a cantilever beam, and the free end was driven by the airfoil connecting rod. Thus, a signal, in phase with the airfoil displacement and hence 180° out of phase with the inertia force of the airfoil, was obtained with the tunnel air turned off, and the inertia signal of the lift bridge could be cancelled at a given frequency.

The frequency of oscillation was determined with a Lissajous circle which was formed on an oscilloscope screen between the inertia signal and a low-frequency oscillator.

A 30-cycle low-pass filter was used to filter objectionable "hash" from the system, and a four-channel recording oscillograph was used with an oscillograph camera for recording the test data.

#### PROCEDURE

The oscillatory lift was recorded at angles of attack ranging from 0° to 28°, at wind velocities ranging from 40 to 240 feet per second, and at frequencies of 11 to 20 cycles per second. The reduced frequency  $k$ , defined by  $k = \omega b/v$  where  $\omega$  is the frequency,  $b$  is the semichord, and  $v$  is the free-stream velocity, varied from 0.06 to 0.5.

At a given angle of attack with no air flowing, the frequency was set; the voltage to the inertia balancing strain-gage bridge was adjusted until the output of the combined systems was zero. The air was then turned on, and records of the oscillatory lift were taken at four or five airspeeds of 50 to 200 feet per second. Similar sets of runs were made at frequencies of 11, 14, 17, and 20 cycles per second; then the airfoil was set to a new angle of attack. Runs were made at each angle of attack with the cascade blades in the tunnel and with them out.

The amplitude of the force and the phase angle between the force and the displacement were read on a film reader. The linear variation of displacement of the airfoil from root to tip was accounted for in the calculation of the force.

## RESULTS AND DISCUSSION

Two quantities are necessary to define the oscillatory lift force: (1) the magnitude of the force as indicated by the strain gages and (2) the phase angle  $\phi$ , which is the angle by which the oscillatory lift force leads the displacement. The damping is positive when  $180^\circ < \phi < 360^\circ$  and negative when  $0 < \phi < 180^\circ$ .

Some typical oscillograph records are shown in figure 3. Part of the data obtained are plotted in figures 4 and 5. Only data taken at 17 and 20 cycles per second are shown, the data at the other frequencies exhibiting similar trends.

The dimensionless lift coefficient  $L_h$  is plotted in figures 4 and 5. This coefficient is given by

$$L = \pi \rho b^2 \omega^2 L_h h$$

where  $L$  is the oscillatory lift force per unit span,  $\rho$  is the air density,  $b$  is the semichord,  $h$  is the displacement, and  $\omega$  is the frequency. The angle of attack plotted is the geometric angle of attack for the isolated airfoil and the vector mean angle, assuming zero deviation, for the cascade. A study of these figures leads to the results presented in the following paragraph.

From figures 4(a) and (b) at zero angle of attack, placing the wing in cascade appears merely to raise the oscillatory lift force and the phase angle slightly. The photographic records also showed that the cascade apparently smoothed out the air flow considerably; that is, the records taken with the cascade in place were much smoother. Nothing of any importance happened as the angle of attack was increased through the stall angle of the airfoil; however, the records made at low frequencies with the single blade became increasingly rough as the angle was increased above the stall. At an angle of attack of  $21^\circ$  for the isolated blade, two blades failed before data could be obtained. Figures 4(c) and (d) show the variation with reduced frequency  $k$  of the oscillatory lift and the phase angle for the isolated airfoil at an angle of attack of  $21^\circ$  and for the airfoil in cascade at an angle of attack of  $22^\circ$ . It can be seen in figure 4(d) that at the highest frequency, 20 cycles per second, the damping becomes negative at low values of  $k$  for the isolated airfoil. Runs were made up to an angle of attack of  $28^\circ$ , and then the runs at the previous conditions were redone. The velocity was slowly increased until the airfoil failed again, and figures 4(c) and (d) were duplicated except at the lowest values of  $k$  where the airfoil failed.

At all angles of attack (fig. 5), the effect of the cascade is to raise slightly the magnitude of the lift force. At angles of attack below  $10^\circ$ , the cascade raises the phase angle  $\phi$ ; at angles of attack above  $10^\circ$ , the cascade has less effect; at angles of attack above  $20^\circ$ , the cascade tends to lower the phase angle at higher frequencies and raises the angle slightly at lower frequencies.

From these same figures it can also be seen that as the angle of attack of the isolated blade is increased, the lift force remains practically unchanged until it starts to fall off at about  $24^\circ$ . When the blade is in cascade, the lift force slowly rises until at a  $28^\circ$  to  $30^\circ$  angle of attack it levels out and possibly starts to drop slightly.

The phase angle for both cases rises to a maximum at an angle of attack of about  $20^\circ$  and then decreases.

Of course, all these data are presented for a reduced frequency of 0.2, but the trends hold true for other values.

The variation of  $L_h$  and  $\phi$  with frequency seems to indicate fairly large Reynolds number effects, at least at low angles of attack. At a reduced-frequency value of 0.2, the Reynolds number varied from 125,000 to 225,000 when the frequency was increased from 11 to 20 cycles per second.

The 30-cycle low-pass filter was necessary to get rid of a large amount of "hash" which was encountered whenever the air was turned on. Undoubtedly this filter removed some harmonics of the oscillatory lift force; therefore, it must be understood that the data presented in this report consist of the fundamental oscillatory lift data.

From the curves presented, it appears that negative damping is definitely possible with an isolated airfoil oscillating in bending. This bears out the experience of Bollay and Brown (ref. 3), who encountered large bending oscillations at angles of attack from  $18^\circ$  to  $24^\circ$ . It also bears out the trend of the data in reference 2. However, the possibility of flutter in bending is lessened, if anything, by placing an oscillating blade in a stationary cascade since at low values of  $k$  and high angles of attack, where the curves of  $\phi$  against  $k$  for the isolated airfoil are tending towards negative damping, the curves for the cascade fall off. This is contrary to the theoretical results set forth in reference 4.

#### SUMMARY OF RESULTS

From the measurements made of the oscillatory force acting on an airfoil vibrated in bending, with the airfoil isolated and in a stationary cascade, the following results were obtained:

1. It is possible for the aerodynamic damping in pure bending to become negative for an isolated airfoil at high angles of attack and at low values of reduced frequency.

2. The effect of placing such an oscillating airfoil in a stationary cascade is not very great for the case of zero stagger and solidity of 2. If anything, the cascade increases the aerodynamic damping.

Lewis Flight Propulsion Laboratory  
National Advisory Committee for Aeronautics  
Cleveland, Ohio, June 30, 1953

6562

#### REFERENCES

1. Mendelson, Alexander: Effect of Aerodynamic Hysteresis on Critical Flutter Speed at Stall. NACA RM E8B04, 1948.
2. Halfman, Robert L., Johnson, H. C., and Haley, S. M.: Evaluation of High-Angle-of-Attack Aerodynamic-Derivative Data and Stall-Flutter Prediction Techniques. NACA TN 2533, 1951.
3. Bollay, William, and Brown, Charles D.: Some Experimental Results on Wing Flutter. Jour. Aero. Sci., vol 8, no. 8, June 1941, pp. 313-318.
4. Bellenot, C., and d'Epina, J. Laline: Self-Induced Vibrations of Turbo-Machine Blades. Brown Boveri Rev., vol. XXXVII, no. 10, Oct. 1950, pp. 368-376.

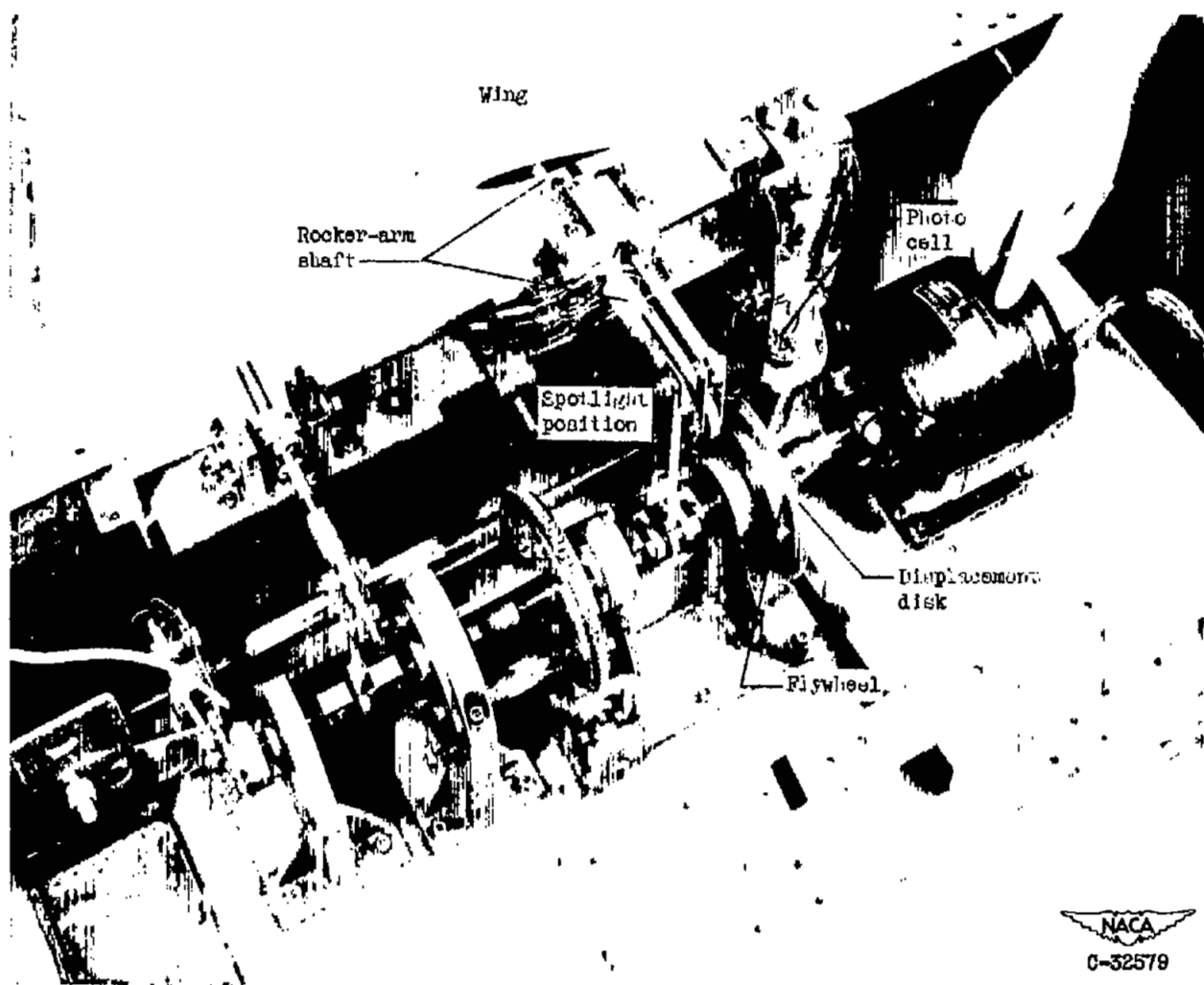


Figure 1. - Flutter engine.

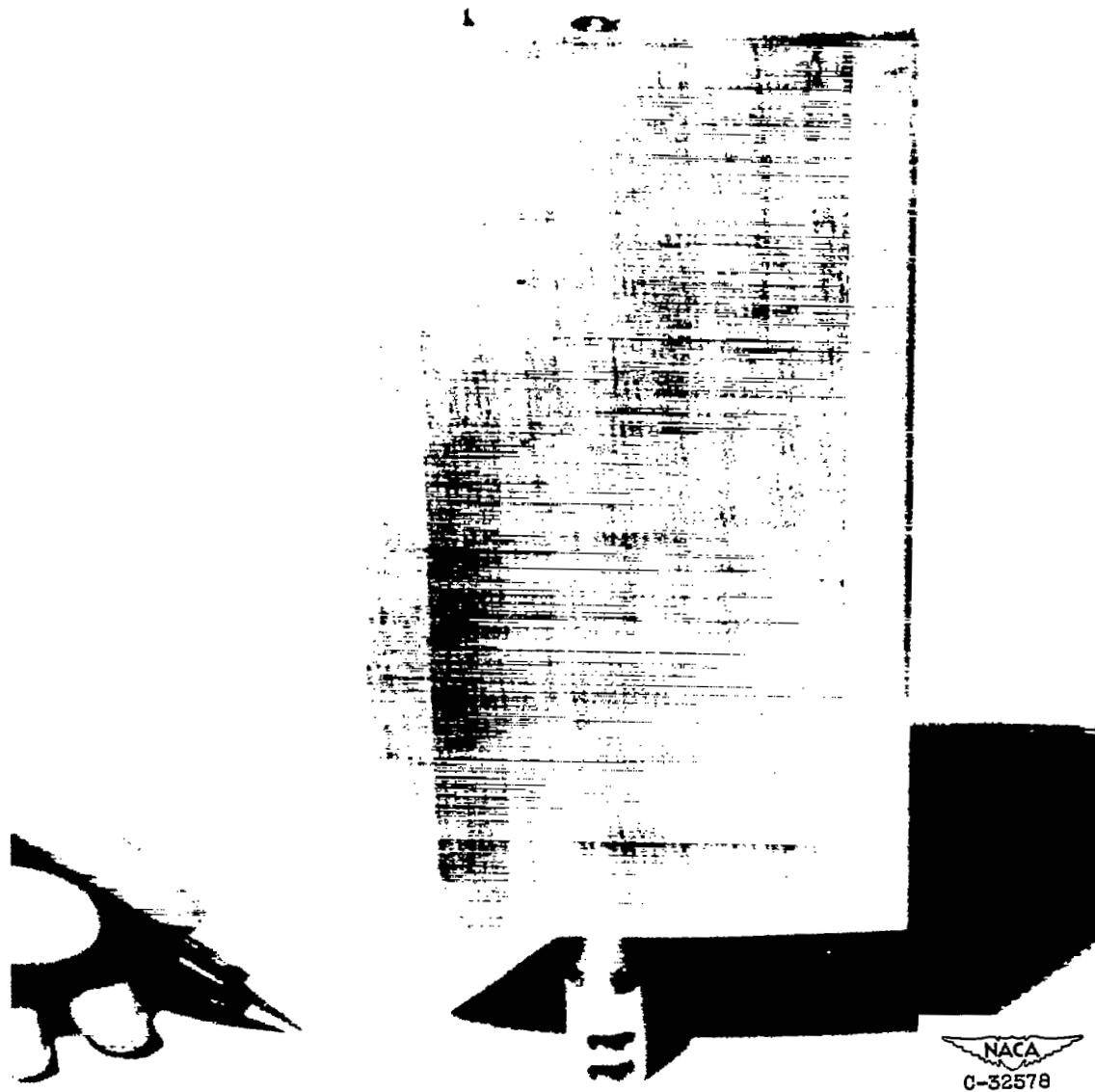
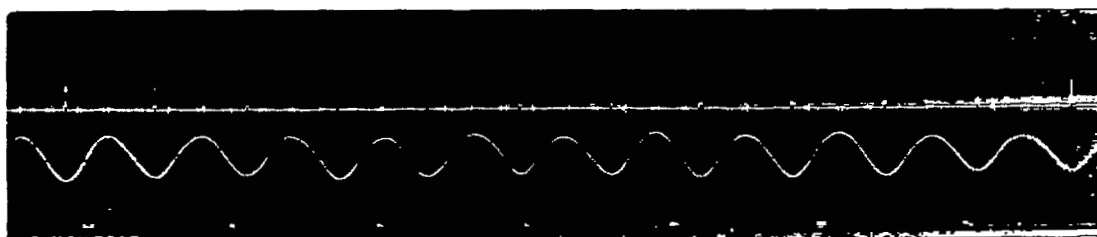


Figure 2. - Model airfoil.

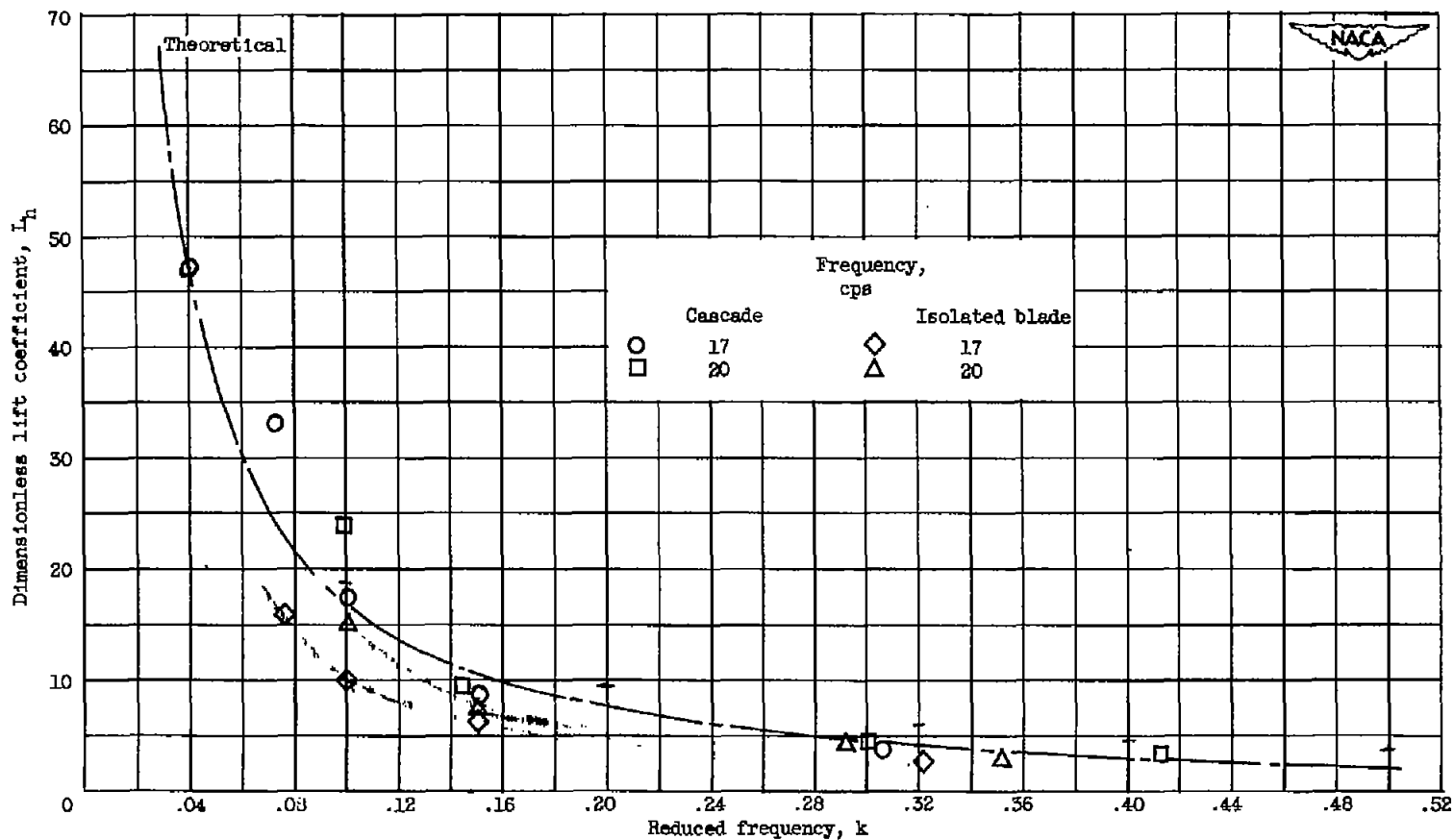
2939

CD-2



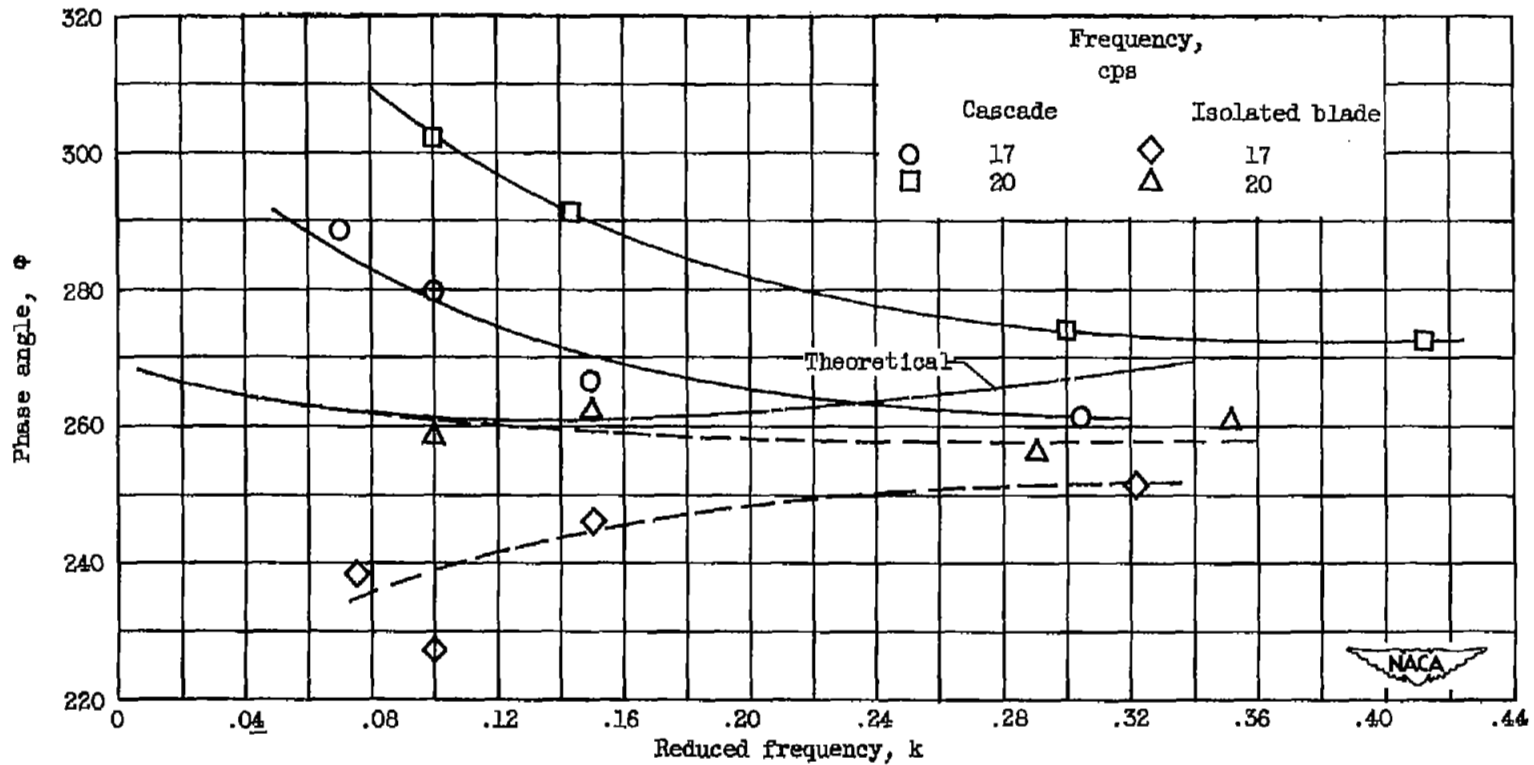
NACA  
C-32785

Figure 3. - Typical record of oscillatory lift force and displacement trace.



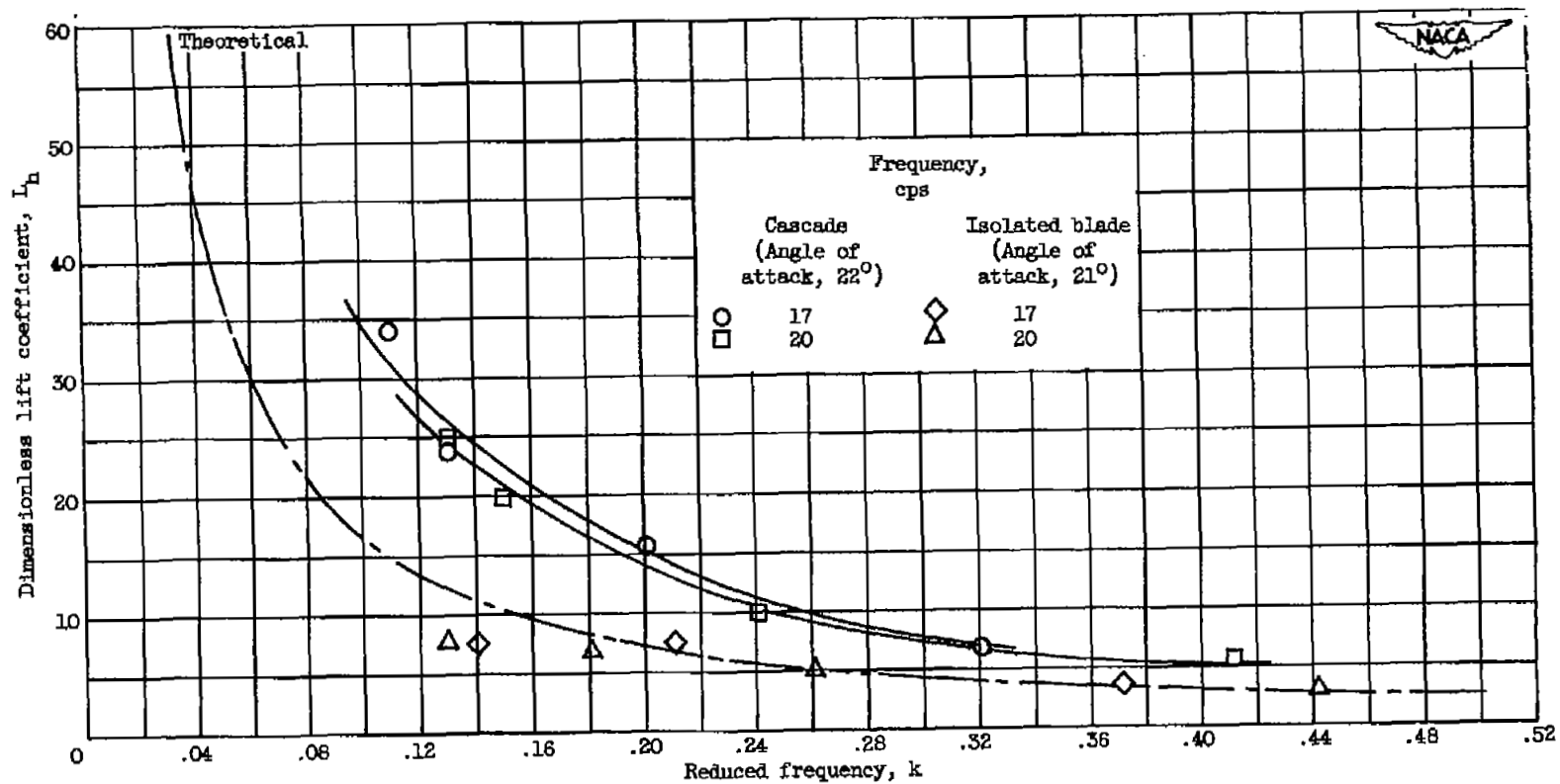
(a) Dimensionless lift coefficient; zero angle of attack.

Figure 4. - Variation of dimensionless lift coefficient and phase angle with reduced frequency.



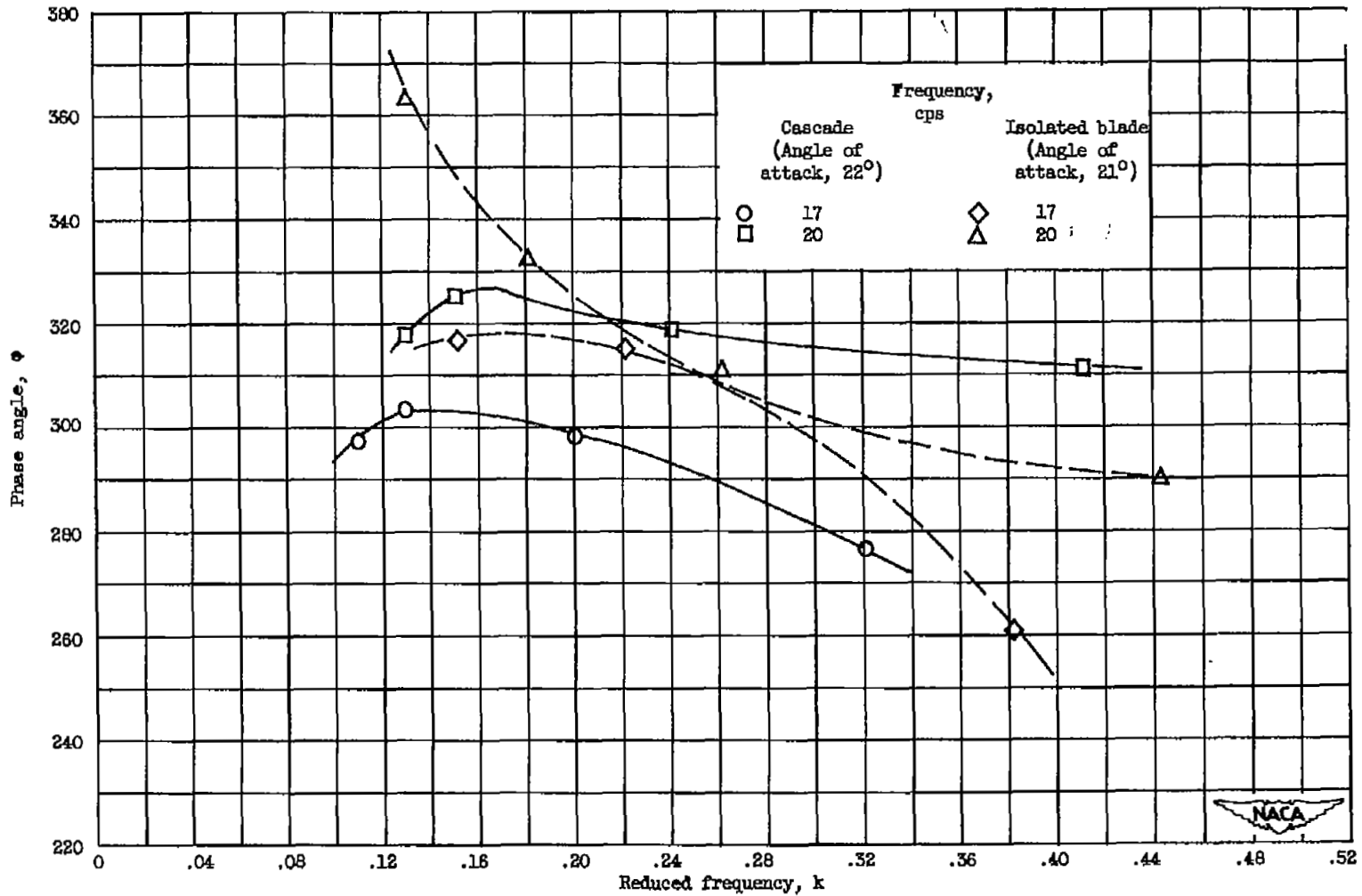
(b) Phase angle; zero angle of attack.

Figure 4. - Continued. Variation of dimensionless lift coefficient and phase angle with reduced frequency.



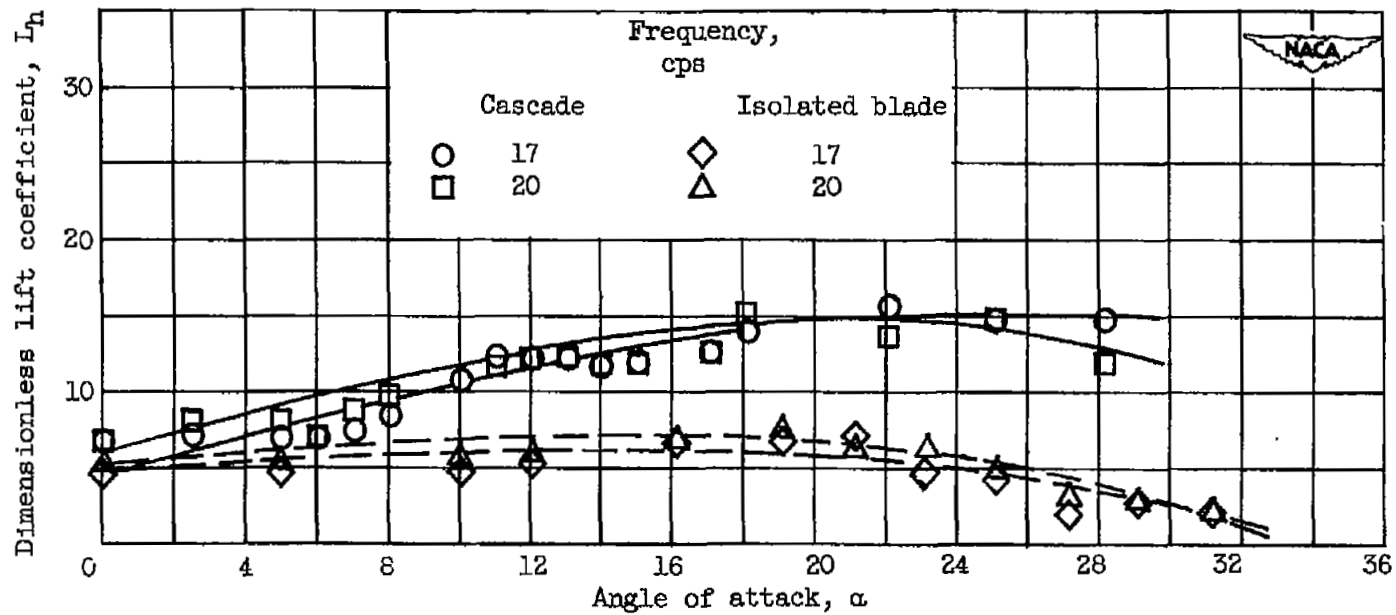
(c) Dimensionless lift coefficient; high angle of attack.

Figure 4. - Continued. Variation of dimensionless lift coefficient and phase angle with reduced frequency



(d) Phase angle, high angle of attack.

Figure 4. - Concluded. Variation of dimensionless lift coefficient and phase angle with reduced frequency.



(a) Dimensionless lift coefficient.

Figure 5. - Variation of dimensionless lift coefficient and phase angle with angle of attack; reduced frequency,  $k$ , 0.2.

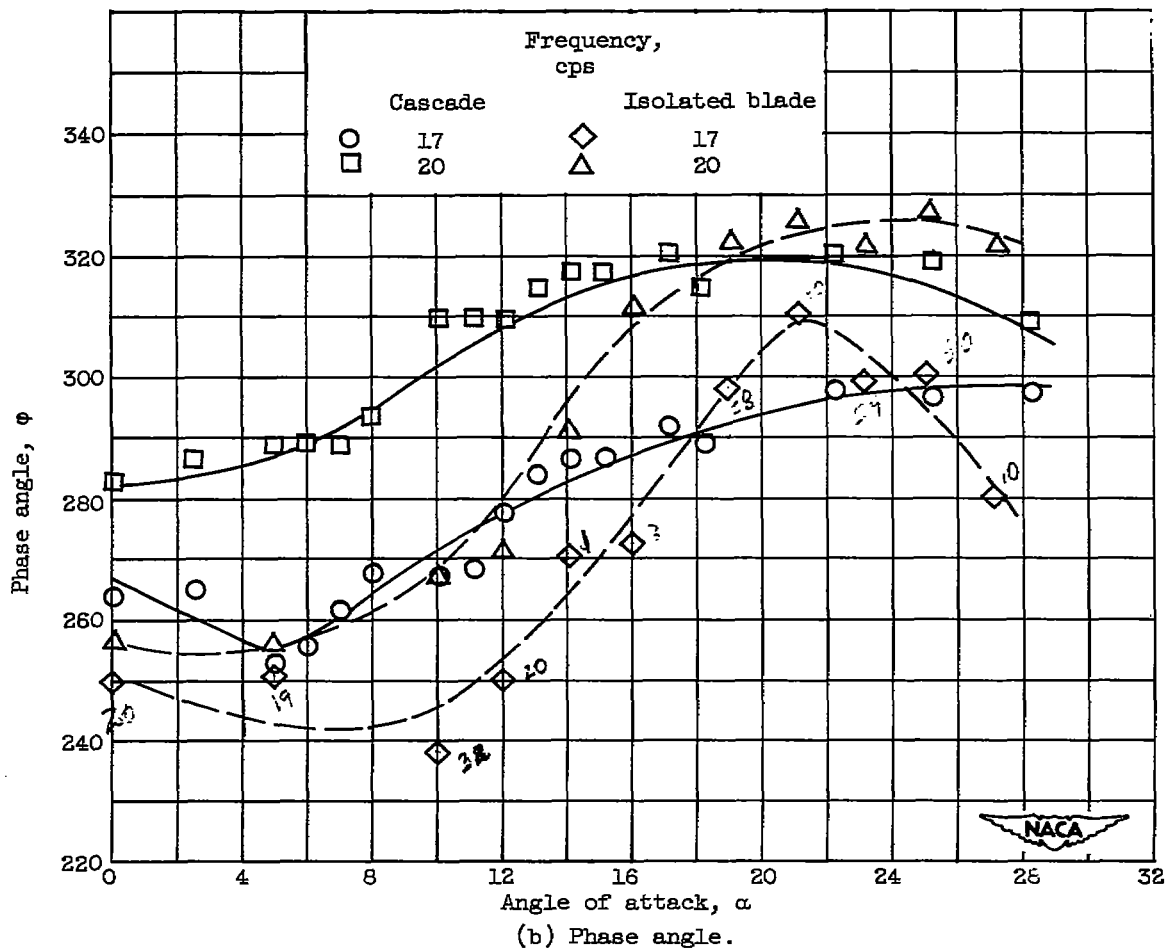
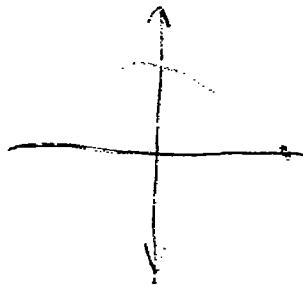


Figure 5. - Concluded. Variation of dimensionless lift coefficient and phase angle with angle of attack; reduced frequency,  $k$ , 0.2.

NASA Technical Library



3 1176 01435 2646